AGU ADVANCING EARTH AND SPACE SCIENCES

Earth's Future

RESEARCH ARTICLE
10.1029/2023EF004129

**Special Section:**
Climate Change, Global Air Quality, and Society

# Comprehensive Impact of Changing Siberian Wildfire Severities on Air Quality, Climate, and Economy: MIROC5 Global Climate Model's Sensitivity Assessments

**Teppei J. Yasunari[1,2], Daiju Narita[3], Toshihiko Takemura[4], Shigeto Wakabayashi[5], and Akira Takeshima[6,7]**

[1]Arctic Research Center, Hokkaido University, Sapporo, Japan, [2]Center for Natural Hazards Research, Hokkaido University, Sapporo, Japan, [3]Graduate School of Arts and Sciences, The University of Tokyo, Tokyo, Japan, [4]Research Institute for Applied Mechanics (RIAM), Kyushu University, Kasuga, Japan, [5]School of Engineering, Hokkaido University, Sapporo, Japan, [6]Center for Environmental Remote Sensing, Chiba University, Chiba, Japan, [7]Institute of Industrial Science, The University of Tokyo, Kashiwa, Japan

**Abstract** Wildfires emit atmospheric aerosols, affecting climate and air quality. Siberia is a known source region of wildfires. However, comprehensive knowledge regarding the impact associated with particulate matter pollution due to Siberian wildfires on climate and air quality and their effects on mortality and the economy under present and near-future warmer atmospheric conditions remains poor. Thus, we performed model sensitivity experiments (atmospheric model and coupled atmosphere-ocean model settings) simulating the effects of changing Siberian wildfire emissions under the present and near-future climate conditions, using the Model for Interdisciplinary Research on Climate version 5 (MIROC5). Increased Siberian wildfire smoke likely caused a cooling effect in broad areas of the Northern Hemisphere and worsened the air quality near the source and in the downwind region (i.e., East Asia). The more Siberian wildfires occur, the more air pollution is present in those regions, which likely increases mortality and welfare losses there. However, the total impact of changing temperature on the gross domestic product under present and near-future climate conditions is ambiguous. Our comprehensive results on the air quality changes due to Siberian wildfires under present and near-future climate conditions suggest that increased efforts to limit the aerosol impact of Siberian wildfires are crucial to prevent possible excess mortality and economic losses.

**Plain Language Summary** Comprehensive knowledge of worsening air quality due to increased Siberian wildfires and its impact on climate and economy is needed to assess the impact of such fires both near their source and in the surrounding regions. Therefore, we performed global climate model simulations and analyzed the changing atmospheric aerosol emissions, including a precursor gas, from Siberian wildfires under the present and near-future climate conditions using the Japanese global climate model called MIROC5. The increased aerosol emissions from Siberian wildfires generated a cooling effect in broad areas of the Northern Hemisphere and worsened the air quality near the source and in the downwind areas of East Asia. The effects we observed are associated with excess mortality and economic welfare losses. Future studies are needed to fully understand and prevent those negative impacts.

**Key Points:**

- Comprehensive impacts of increasing Siberian wildfires on air quality, climate, and economy were estimated using the MIROC5 climate model
- We observed a cooling effect broadly across the Northern Hemisphere and worsened air quality near wildfire source and downwind regions
- The effects are closely related to lowering achievement rates of $PM_{2.5}$ environmental standards, excess mortality, and economic losses

**Supporting Information:**

Supporting Information may be found in the online version of this article.

**Correspondence to:**

T. J. Yasunari,
t.j.yasunari@arc.hokudai.ac.jp

**Citation:**

Yasunari, T. J., Narita, D., Takemura, T., Wakabayashi, S., & Takeshima, A. (2024). Comprehensive impact of changing Siberian wildfire severities on air quality, climate, and economy: MIROC5 global climate model's sensitivity assessments. *Earth's Future*, *12*, e2023EF004129. https://doi.org/10.1029/2023EF004129

Received 25 SEP 2023
Accepted 23 MAR 2024

**Author Contributions:**

**Conceptualization:** Teppei J. Yasunari, Daiju Narita, Toshihiko Takemura, Shigeto Wakabayashi
**Data curation:** Teppei J. Yasunari, Daiju Narita, Toshihiko Takemura, Akira Takeshima
**Formal analysis:** Teppei J. Yasunari, Daiju Narita



## 1. Introduction

Wildfires occur every day, season, and year at various places (Darmenov & da Silva, 2015; Pan et al., 2020). Human and natural ignitions cause wildfires (Amatulli et al., 2007; Narita et al., 2021; Rodrigues & de la Riva, 2014) (also see NASA's Fire Information for Resource Management System (FIRMS) at https://firms.modaps.eosdis.nasa.gov/). Wildfire activities are relevant to atmospheric aerosols, air pollution, human health, climate, and the economy as mentioned below.

Large-scale wildfires are of considerable concern owing to their significant impact on large forested and vegetated areas and/or human lives if the people live in the surrounding areas, such as the cases of wildfires in California in the US (Westerling & Bryant, 2008). Because large-scale wildfires also emit massive amounts of air pollution, such as carbonaceous aerosols (Yasunari et al., 2018), causing higher $PM_{2.5}$ levels (Yasunari et al., 2022), the impact of wildfires on human health is a considerable concern. The scale of wildfires largely depends on the climate and environmental conditions in the source areas (e.g., Westerling et al., 2006; Yasunari et al., 2018,

**Funding acquisition:** Teppei J. Yasunari, Daiju Narita, Toshihiko Takemura
**Investigation:** Toshihiko Takemura
**Methodology:** Teppei J. Yasunari, Daiju Narita, Toshihiko Takemura, Shigeto Wakabayashi
**Project administration:** Teppei J. Yasunari
**Resources:** Toshihiko Takemura, Akira Takeshima
**Software:** Teppei J. Yasunari, Toshihiko Takemura, Akira Takeshima
**Supervision:** Teppei J. Yasunari
**Validation:** Teppei J. Yasunari, Daiju Narita, Toshihiko Takemura
**Visualization:** Teppei J. Yasunari, Daiju Narita
**Writing – original draft:** Teppei J. Yasunari, Daiju Narita
**Writing – review & editing:** Teppei J. Yasunari, Daiju Narita, Toshihiko Takemura

2021). Increased mortality was reported in the case of interaction between heatwaves and wildfire air pollution in 2010 in Moscow, Russia (Shaposhnikov et al., 2014). Ambient air pollution is one of the top global health risks (GBD 2015 Risk Factors Collaborators, 2016), and the World Health Organization (WHO) estimated that approximately 4.2 million people lost their lives in 2019 because of ambient air pollution (https://www.who.int/news-room/fact-sheets/detail/ambient-(outdoor)-air-quality-and-health). A comprehensive global study on the relationship between ambient air pollution and premature mortality indicated that the air pollution in Siberia due to biomass burning (BB) (i.e., wildfires) contributes markedly to premature mortality (Lelieveld et al., 2015). A recent study reported that $PM_{2.5}$ originating from wildfires increased respiratory hospitalization compared to other $PM_{2.5}$ sources (Aguilera et al., 2021).

Such health effects of ambient air pollution from BB also have economic implications, and the economic costs of ambient air pollution are estimated to be substantial, equivalent to welfare losses of several percent of gross domestic product (GDP) in the most affected regions (Landrigan et al., 2018; World Bank & Institute for Health Metrics and Evaluation, 2016). As a specific example of assessing the economic impact of wildfires, Kochi et al. (2012) estimated that the southern California wildfire in 2003 induced a loss of approximately 1 billion US dollars due to smoke exposure based on 133 excess cardiorespiratory-related deaths. The more recent 2018 wildfires in California were economically assessed by Wang et al. (2021) who concluded that the total damage due to the wildfires amounted to 148.5 billion US dollars that year. In addition to direct impact on human health, air pollution from wildfires can also affect the economy and society through climatic effects. Atmospheric aerosol emissions and depositions from wildfires, such as black carbon, can change atmospheric and snow radiation budgets, meaning that wildfires also contribute to changing climate regionally and globally via feedback (Flanner et al., 2009; Liu et al., 2014 and references therein; Yan et al., 2021). Based on recent scholarship on the economic assessment of climate change impact (e.g., Burke et al., 2018; Dell et al., 2012; National Academies of Sciences, Engineering, and Medicine, 2017), some attempts have been made to assess the macroeconomic impact of the climatic effects of air pollution (Scovronick et al., 2019; Shindell, 2015; WHO & UNEP, 2011; Zheng et al., 2020). However, these studies did not specifically examine the impact of air pollution from wildfires.

Wildfire is not only of considerable concern under present climate conditions but will be of greater concern in the future. A recent study has projected a higher number of wildfires under future conditions owing to climate change along with the associated air pollution emissions (Veira et al., 2016). Furthermore, even the latest six assessment reports (AR6) of the Intergovernmental Panel on Climate Change (IPCC) (IPCC, 2021) stated that fire weather would increase (with medium to high confidence) in specific regions under future climate change. Therefore, comprehensive assessments of the impact of wildfire on air quality, climate, human health, and economy are needed to determine the correct steps to sustain human existence in the future.

Siberia is one of the many regions where large-scale wildfires have been frequently observed (Pan et al., 2020). It is challenging to extinguish fires in Siberia owing to its large area. In recent years, the co-occurrence of wildfires in Siberia and sub-polar North America (Alaska and Canada) in the summer season was reported when the air pollution level was relatively higher in the Arctic, which might be explained by the recent change in the climate pattern in the atmosphere (Yasunari et al., 2021). In the present study, we assessed the impact of increased wildfires over Siberia on air pollution, mortality, economy, and present and near future (2030) climate conditions especially from Siberia to the downwind region in East Asia and remote regions (e.g., Europe and North America). Six numerical sensitivity experiments were conducted using a global climate model (GCM) developed in Japan. We mostly used the outputs for the analyses from the coupled Atmosphere and Ocean GCM (AOGCM) experiments in this study, except for the analyses of the instantaneous aerosol radiative forcing (IARF) and effective radiative forcing (ERF) (Forster et al., 2016; Myhre et al., 2013) for the Atmospheric GCM experiments (AGCM). To assess the impacts of increased Siberian wildfires on air quality, climate, and economy under present and near-future climate conditions, we performed six experiments with different biomass burning emissions and greenhouse gas (GHG) concentrations using AGCM and AOGCM experiments. Using the estimation functions proposed in recent literature, we discuss the air pollution and climatic impact on mortality and economic output due to increased Siberian wildfires under the present and near-future climate conditions. Note that for the GCM sensitivity experiments under the near-future climate conditions, we focused more on the combined effect of Siberian wildfires and global warming rather than each effect individually, because it is crucial to provide a quantitative view of the total effect from the perspective of temperature.

## 2. Materials and Methods

### 2.1. Global Simulations and Data Analyses

To investigate the sensitivities of increasing Siberian wildfires in the present and near future (i.e., in 2030), we conducted global sensitivity simulations using the AGCM and AOGCM. We used a climate model developed in Japan (MIROC: Model for Interdisciplinary Research on Climate; version 5.9.0; known as MIROC5: Watanabe et al., 2010) with its aerosol module, Spectral Radiation-Transport Model for Aerosol Species (SPRINTARS; https://sprintars.riam.kyushu-u.ac.jp/indexe.html) (Takemura et al., 2000, 2002). We selected 2030 for the near-future climate condition because 2030 is of considerable concern to the general public at the end of the well-known Paris Agreement (https://unfccc.int/process-and-meetings/the-paris-agreement), and this would be important from an economic perspective. We used a horizontal grid spacing of T85 (approximately 1.4° × 1.4° in longitude and latitude) with vertical resolution of L40 (40 vertical layers). For the AGCM and AOGCM experiments, we implemented 15 and 100 years of integration in the simulations as equilibrium experiments: we can analyze multi-year averages of equilibrium conditions in which we account for internal climate variability even under the same BB emissions. Then, we analyzed the last 10 and 50 years, respectively (considering the climate conditions reach equilibrium). The model simulation data with scripts for analyses and the other data used in this study, except for some data mentioned in the other parts of the main text, are available in Yasunari et al. (2024). To assess increased Siberian wildfires, we chose the years 2004 and 2003 as a baseline case (fewer wildfires) and high BB emission case (more wildfires), respectively: the Siberian fire characteristics of those years have been reported, for example, in Figure 9 from Darmenov and da Silva (2015).

Daily BB emissions were obtained from the Global Fire Emission Database (GFED; version 3.1, hereafter called GFEDv3.1; https://www.globalfiredata.org/) (Randerson et al., 2013; van der Werf et al., 2010). As Figure 9 from Darmenov and da Silva (2015) reported, GFEDv3.1 BB emissions tend to be lower than those of other BB emission inventories. We also checked the time series of the BB emissions over the defined Siberian domain (70°E–140°E; 42.5°N–70°N) with the GFEDv3.1 BB emission data during 2003 and 2010 (Figure S1 in Supporting Information S1). Then, we confirmed that 2004 and 2003 were the representative years of low background and high emission cases, respectively. Our study focused on air quality and its impact on mortality and the economy, so lower-bound estimates are generally better than upper-bound estimates to avoid overvaluation. Therefore, these data can be used to discuss how much the increased Siberian wildfires would at least impact climate, air quality, human health, and the economy. Furthermore, our simulations replace BB emissions over the defined Siberian domain to the one in 2003 or doubling the one in 2003. Therefore, comparing $PM_{2.5}$ in a specific year between our results and observations is very difficult. However, the quality of the simulated $PM_{2.5}$ due to Siberian wildfires using GFEDv3.1 was already reported by Ikeda and Tanimoto (2015). Their modeled results reasonably reproduced the time-varying $PM_{2.5}$ observed at a few sites in Japan. Given the above information, we considered GFEDv3.1 to be a reasonable source of data for our study. Also, we check the performance of the simulated $PM_{2.5}$ with the other data set, as mentioned below.

To compare different climatic conditions, the following conditions were selected: One present climate (the initial condition in 2005 was mainly used, except for the BB settings). Two different near-future climate conditions are based on RCP scenarios in terms of GHG concentrations (RCP in 2005 for the present climate, and RCP2.6 and 8.5 for the near-future climate conditions in 2030). Except for the following conditions of the BB aerosol emissions, the other aerosol emissions were based on the present climate condition (RCP in 2005) for all the experiments. Six AGCM and AOGCM experiments were conducted, respectively (see the model settings on BB emissions and GHG concentrations in Table 1).

Most analyses were performed using outputs from AOGCM experiments. However, the AGCM outputs were also used to calculate IARF and ERF. For ERF, radiation differences need to be calculated under unchanged surface conditions, such as a fixed sea surface temperature, as defined in the Fifth Assessment Report (AR5) (Myhre et al., 2013) of the IPCC.

Although our global simulations were unique, changing the Siberian BB emissions makes it difficult to validate the simulated $PM_{2.5}$ against available observations (namely, difficulty in apple-to-apple comparisons). However, we implemented what we could do best on the comparisons. We decided to use the data-assimilated data set (DAD) of $PM_{2.5}$ for the comparisons (V5.GL.04 in 0.1°×0.1° horizontal resolution: https://sites.wustl.edu/acag/datasets/surface-pm2-5/#V5.GL.04): in the data set, observations (satellite-retrieved and monitor-based data) and

**Table 1**
*MIROC5/SPRINTARS AGCM and AOGCM Experiment Settings on Biomass Burning (BB) Emissions and Greenhouse Gases (GHG) Concentrations*

| Experiment ID | Daily GFED BB emission condition (BC, OC, and $SO_2$)[a] | GHGs concentrations | Note |
|---|---|---|---|
| EXP0 | BB emission in 2004 | RCP in 2005[b] | Control case under the present climate condition (low Siberian BB emissions) |
| EXP1 | BB in 2004, but the BB in 2003 over the defined Siberian domain | RCP in 2005[b] | High Siberian BB emission case under the present climate condition |
| EXP2 | BB in 2004, but the BB × 2 in 2003 over the defined Siberian domain | RCP in 2005[b] | Doubling the high Siberian BB emission case under the present climate condition |
| EXP3 | BB in 2004, but the BB in 2003 over the defined Siberian domain | RCP2.6 in 2030[b] | High Siberian BB emission case but GHG concentrations in 2030 with RCP2.6 |
| EXP4 | BB in 2004, but the BB × 2 in 2003 over the defined Siberian domain | RCP2.6 in 2030[b] | Doubling the high Siberian BB emission case but GHG concentrations in 2030 with RCP2.6 |
| EXP5 | BB in 2004, but the BB × 2 in 2003 over the defined Siberian domain | RCP8.5 in 2030[b] | Doubling the high Siberian BB emission case but GHG concentrations in 2030 with RCP8.5 |

[a]van der Werf et al. (2010) and Randerson et al. (2013). [b]Moss et al. (2010) and van Vuuren et al. (2011).

chemical transport modeled data were combined to reflect better global $PM_{2.5}$ variations between 1998 and 2022 by the method of van Donkelaar et al. (2021). Namely, this DAD is the best data set for comparisons with the simulated $PM_{2.5,}$ reflecting many available observations. We merged all the monthly mean data (DAD) files into a single file (see the merged data in Yasunari et al. (2024)).

To assess the achievement rates of short-term air quality in some countries and Russian administrative divisions, which should be affected by temporal wildfire smoke variations, we used the daily mean $PM_{2.5}$ and environmental standard (ES) of 15 μg $m^{-3}$, which was recently determined by the WHO (WHO, 2021). The achievement rate of $PM_{2.5}$ is also used in Japan (https://www.env.go.jp/content/900514658.pdf). The gridded $PM_{2.5}$ data from the AOGCM outputs were spatially averaged over the countries and administrative divisions (Figure S2 in Supporting Information S1) with population weighting using the population data provided by the Shared Socioeconomic Pathways (SSP) (Riahi et al., 2017) (Version 1.0; https://secure.iiasa.ac.at/web-apps/ene/SspDb/dsd?Action=htmlpage&page=10). The SSP population data were re-gridded to T85 spatial resolution using SPRING (SPheroidal coordinates Regridding INterpolation table Generator; preliminary version; http://hydro.iis.u-tokyo.ac.jp/~akira/page/Works/contents/SPRING/). The population and other socioeconomic data under the present climate use the baseline year of 2010 in this study. We also used the annual mean $PM_{2.5}$ data to assess the mean differences for the selected countries and divisions for economic analyses.

### 2.2. Estimated Mortality and Economy-Wide Impacts of Increased Siberian Wildfires

Enhanced particulate emissions through the intensification of Siberian wildfires can have various economic impacts. In the present study, we attempted to quantify two kinds of impacts, namely those associated with increased premature mortality through exposure to ambient fine particulate matter ($PM_{2.5}$) and climate change, both evaluated in terms of welfare losses. Based on the data of the OECD's long-term GDP forecasts, we estimate welfare impact in terms of the 2003–2017 average GDP and the 2030 GDP projections. The economic consequences of wildfires are not limited to these two factors and may also be associated with other factors, notably the morbidity associated with air pollution. However, an earlier assessment (World Bank & Institute for Health Metrics and Evaluation, 2016) suggested that, in the context of ambient air pollution, the costs of mortality may generally dominate the costs of morbidity when expressed as welfare loss. Moreover, recent studies on the economic effects of particulate emissions focused on their mortality and climatic effects (Scovronick et al., 2019; Shindell, 2015; Zheng et al., 2020).

In terms of pollution impacts on mortality and the economy, the model outputs of population-weighted averages of the annual surface $PM_{2.5}$ concentrations were used to estimate excess premature mortality from enhanced air pollution due to the intensification of wildfires. We conducted estimations for China, South Korea, Japan, and five Russian areas (Amur, Zabaykal'ye, Buryat, Khabarovsk, and Irkutsk). Note that here, we only considered the impact of $PM_{2.5}$ and not ozone and other non-PM air pollutants. To link pollution exposure and mortality, we used the Global Exposure Mortality Model (GEMM) (Burnett et al., 2018), which is formulated as:

$$RR(z) = \exp\left[\frac{\theta \cdot \ln(1 + z/\alpha)}{1 + \exp\left(-\frac{z-\mu}{\nu}\right)}\right],$$

$$z = \max[0, \mathrm{PM}_{2.5} - z_{cf}],$$

where $RR$ is the relative risk of premature mortality due to exposure to ambient $PM_{2.5}$, $PM_{2.5}$ is the exposure level of $PM_{2.5}$, $z_{cf}$ is the counterfactual concentration level below which no additional risk is assumed, and $\theta$, $\alpha$, $\mu$, and $\nu$ are parameters. We adopted the parameterization of Burnett et al. (2018) for aggregate mortality from all non-communicable diseases and lower respiratory infections induced by ambient $PM_{2.5}$ air pollution (estimates inclusive of the Chinese male cohort data).

For alternative estimations, we also utilized the Integrated Exposure-Response (IER) model (Burnett et al., 2014), which is an earlier model than the GEMM (Burnett et al., 2018). The IER model is generally regarded as less state-of-the-art than the GEMM model because of its limited applicability to cases of high-level pollution exposure (Zheng et al., 2021). Thus, we present our GEMM estimates as the primary results. However, as the IER model was developed earlier, it has been widely used for quantifying the health impact of air pollution (e.g., Cohen et al., 2017; Lelieveld et al., 2015; Seposo et al., 2019). Specifically, the IER model described by Burnett et al. (2014) is represented by probabilistic distributions of parameters composed of 1,000 possible levels. We adopted the median estimate of the computations using these 1,000 sets of parameters.

In the IER framework (Burnett et al., 2014), enhanced mortality risk due to pollution exposure is formulated using the following functions of relative risk:

$$RR(\mathrm{PM}_{2.5}) = \begin{cases} 1 + \alpha\left\{1 - \exp\left[-\gamma(\mathrm{PM}_{2.5} - z_{cf})^{\delta}\right]\right\} & (\mathrm{PM}_{2.5} > Z_{cf}) \\ 1 & (\mathrm{PM}_{2.5} \le Z_{cf}) \end{cases},$$

where $\alpha$, $\gamma$, and $\delta$ are the parameters. We adopted the parameter estimates reported by Burnett et al. (2014). The relative risk considered here is a composite of the RRs for the following illnesses: lung cancer (for all ages), chronic obstructive pulmonary disease (for all ages), ischemic heart disease (age group-specific), stroke (age group-specific), and acute lower respiratory infections (for children aged 0–4 years).

The excess mortality $\Delta M$ was estimated from the relative risk and baseline mortality $M$ according to the following equation:

$$\Delta M = \frac{RR - 1}{RR} M.$$

We used cause-specific mortality data by country and age group from the Global Burden of Disease Study 2017 (GBD 2017 SDG Collaborators, 2018) of the Institute for Health Metrics and Evaluation (IHME). In addition, data on estimates and projections of population and age-group-specific life expectancy were drawn from the World Population Prospects 2019 data by the United Nations (https://www.un.org/development/desa/pd/news/world-population-prospects-2019-0).

For Russian sub-national administrative units, we scaled federal-level data of long-term economic forecasts and case-specific mortality rates using the mortality data from the Centre for Demographic Research at the New Economic School (http://demogr.nes.ru/en/demogr_indicat/data) and the economic data of the Russian Federal State Statistic Service (https://rosstat.gov.ru). Those data used in this study were archived in the data repository in Yasunari et al. (2024).

The increase in mortality estimated using the GEMM (Burnett et al., 2018) and IER (Burnett et al., 2014) models was converted to economic welfare loss based on the value of statistical life (VSL) framework, representing the sum of individuals' willingness to pay (WTP) for marginal changes in their mortality risk (for the information about the concept, see World Bank & Institute for Health Metrics and Evaluation, 2016). The WTP value could, in principle, differ in different contexts (e.g., countries), and ideally, the values could be estimated from context-

specific surveys of different populations. As most countries in the world lack such survey data, we employed the benefit transfer approach (i.e., finding estimates by transferring available information of studies in another location) used by the World Bank and the IHME (World Bank & Institute for Health Metrics and Evaluation, 2016) and Narain and Sall (Narain & Sall, 2016), which estimate VSL using the following functional form:

$$\mathrm{VSL}_{i,t} = \mathrm{VSL}_{\mathrm{Base}} \left( \frac{y_{i,t}}{y_{\mathrm{Base}}} \right)^{\epsilon},$$

where $\mathrm{VSL}_{i,t}$, $\mathrm{VSL}_{\mathrm{Base}}$, $y_{i,t}$, and $y_{\mathrm{Base}}$ are the VSL for country $i$ in year $t$, the base VSL, the income level (GDP per capita at purchasing power parity, PPP) for country $i$ in year $t$, and the base income level, respectively. The base VSL ($3.83 million in 2011 USD at PPP) is the mean level of WTP estimates from surveys conducted in the OECD countries, whose average income level is the base income level (approximately $37,000 in 2011 USD at PPP). Following the World Bank and IHME (World Bank & Institute for Health Metrics and Evaluation, 2016), the elasticity $\epsilon$ is set to be 0.8 for Japan and South Korea (high-income economies) and 1.2 for others.

Additionally, we conducted alternative estimations of welfare loss from BB-related air pollution based on the value per statistical life year (VSLY), which is the value of a 1-year reduction in life expectancy. Similar to the VSL estimations, we applied the benefit transfer method to compute VSLY for different countries and years and used the estimate of the base VSLY by Narain and Sall (2016), which was approximately $190,000 in 2011 USD at PPP.

This study used a similar approach to Zheng et al.'s (2020) economic evaluation of the climatic effects of aerosols and drew on the empirical response function of economic growth to temperature developed by Burke et al. (2018). The Burke et al.'s function is a representation of the statistical relationship between the past levels of GDP and temperatures across world nations, which are based on national and annual averages of economic and climatic data for 165 countries over the period 1960 to 2010 (see Equation 1 of Burke et al. (2018)). We evaluated the potential scale of the macroeconomic impact of Siberian wildfires' climatic effects by drawing on the results of sensitivity experiments on enhanced BB emissions over the defined Siberian domain using the MIROC5/SPRINTARS AOGCM sensitivity simulations (see Section 2.1). The differentials of the annual population-weighted area-average temperatures at 2 m from the simulations over the countries and administrative divisions (Figure S2 in Supporting Information S1) were used to compute the monetary-equivalent economic impact attributable to the climatic effects of BB. Finally, the country-average temperature changes were used to estimate the resultant economic impact (welfare losses expressed as a share of GDP).

## 3. Results

### 3.1. Estimated Mortality Due To Worsened Air Quality Caused by the Siberian Wildfires

First, we compared our simulated $PM_{2.5}$ to the observation-reflected DAD in the focused regions in and around the Siberian domain from spring to summer to understand the model's performance (Figure S3 in Supporting Information S1). On the control simulation (EXP0; i.e., low BB emission case), using the BB emission data in 2004, the $PM_{2.5}$ patterns were well reproduced, though the simulated $PM_{2.5}$ underestimated that of some areas (Figures S3a and S3b in Supporting Information S1). Next, the increased BB emission case over the Siberian domain (EXP1) also captured the $PM_{2.5}$ distributions over the Siberian region well, though again, the magnitude was somewhat underestimated (Figures S3c and S3d in Supporting Information S1). These results confirm that our simulations can reasonably capture the $PM_{2.5}$ distributions from the BB emissions from the Siberian region. The underestimated $PM_{2.5}$ in our simulations on magnitude also supports that our study can suggest that we can discuss the lower-bound estimate of $PM_{2.5}$ impact on air quality, human health, and the economy in this study based on the sensitivity experiments.

Under the present climatic conditions, the AOGCM sensitivity experiments in EXP1 and EXP2 showed increased $PM_{2.5}$ of greater than 20 μg $m^{-3}$ in the fire areas, mainly from spring to summer (April–July) over the Siberian region (Figure 1 and Figure S4 in Supporting Information S1). In this study, the highest increase was seen in May. In the 50-year climatology, $PM_{2.5}$ also increased in the North Pacific region (i.e., downwind of the Siberian region) when Siberian wildfires were active. We used the same present BB emissions applied to the near-future condition (Table 1). Therefore, the patterns of $PM_{2.5}$ distribution looked similar in 2030 (Figure S5 in Supporting

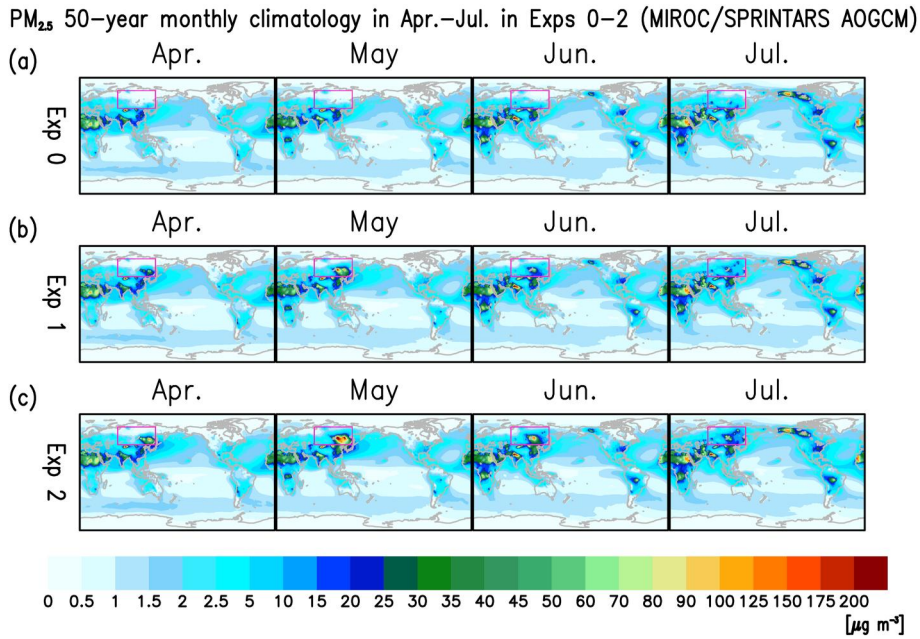


**Figure 1.** Fifty-year monthly surface $PM_{2.5}$ climatology from the AOGCM experiments during April and July for EXPs 0–2 under the present climate conditions.

Information S1). Based on the sensitivity experiments, the most affected areas due to the increased $PM_{2.5}$ were the eastern part of Lake Baikal and its downwind region.

To assess the impact of the worsened short-term air quality due to the increased Siberian wildfires on human health, we analyzed the percentage of the achievement rates of daily mean $PM_{2.5}$ levels in each selected East Asian country (China, South Korea, and Japan) and Russian administrative districts located in the downwind regions from the Siberian wildfire source areas using the ES. We used the new daily mean $PM_{2.5}$ ES of 15 μg $m^{-3}$ (WHO, 2021), which was recently updated from "Global update 2005" by the WHO (WHO Occupational and Environmental Health Team, 2006). Under the present climate conditions in which the $PM_{2.5}$ data were weighted with the 2010 SSP population (Riahi et al., 2017), in South Korea, Japan, and the selected Russian administrative districts, percentages of the achievement rates for the short-term air quality in EXP1 were 77.4%–94.7%. For China in EXP1, however, this was 1.4% (Figure 2). Furthermore, doubling the Siberian wildfire emissions of EXP1 (i.e., EXP2) further decreased the achievement rate percentages by 71.7%–90.2% except for China. The one for China was mostly similar (1.2%) to that in EXP1. Compared to the lowest wildfire emission case in the Russian administrative districts (EXP0; achievement rate percentages >98.2%), notable decreases were seen based on the observed high-emission wildfire case in 2003. Compared with the cases for the Russian administrative districts, the changes in the achievement rate percentages in China, South Korea, and Japan were smaller (Figure 2). However, the percentage of the achievement rates was already extremely low in China (<2.4%), even in the low wildfire emissions case (EXP0). These percentages in China slightly decreased because of additional dominant contributions from the increased Siberian wildfire emissions (EXP1 and EXP2). In remote regions, compared to EXP0, 7.4% and 3.9% decreases in EXP1 (12.4% and 8.4% in EXP2) were likely in South Korea and Japan, respectively. Those achievement rate percentages satisfying the daily mean ES were further reduced (Figure S6 in Supporting Information S1) when we only focused on the main fire seasons from spring to summer (from March to August) when the Siberian wildfires were active (Darmenov & da Silva, 2015; Ikeda & Tanimoto, 2015; Yasunari et al., 2018). When we focused on long-term (i.e., annual mean) air quality for those selected countries and Russian administrative districts, the annual mean $PM_{2.5}$ mass concentrations of the increased Siberian wildfire case (EXP1) and its doubled case (EXP2) were also significantly higher than those of the baseline case (EXP0) (Figure S7 in Supporting Information S1). Those annual mean differences were much more prominent in the Amur, Zabaykal'ye, and Buryat regions in Russia. These results imply that the impact of the increased Siberian wildfire emissions from near the wildfire sources to the remote countries in downwind regions cannot be ignored. Under the 2030 near-future climate conditions, the characteristics of the achievement

10.1029/2023EF004129

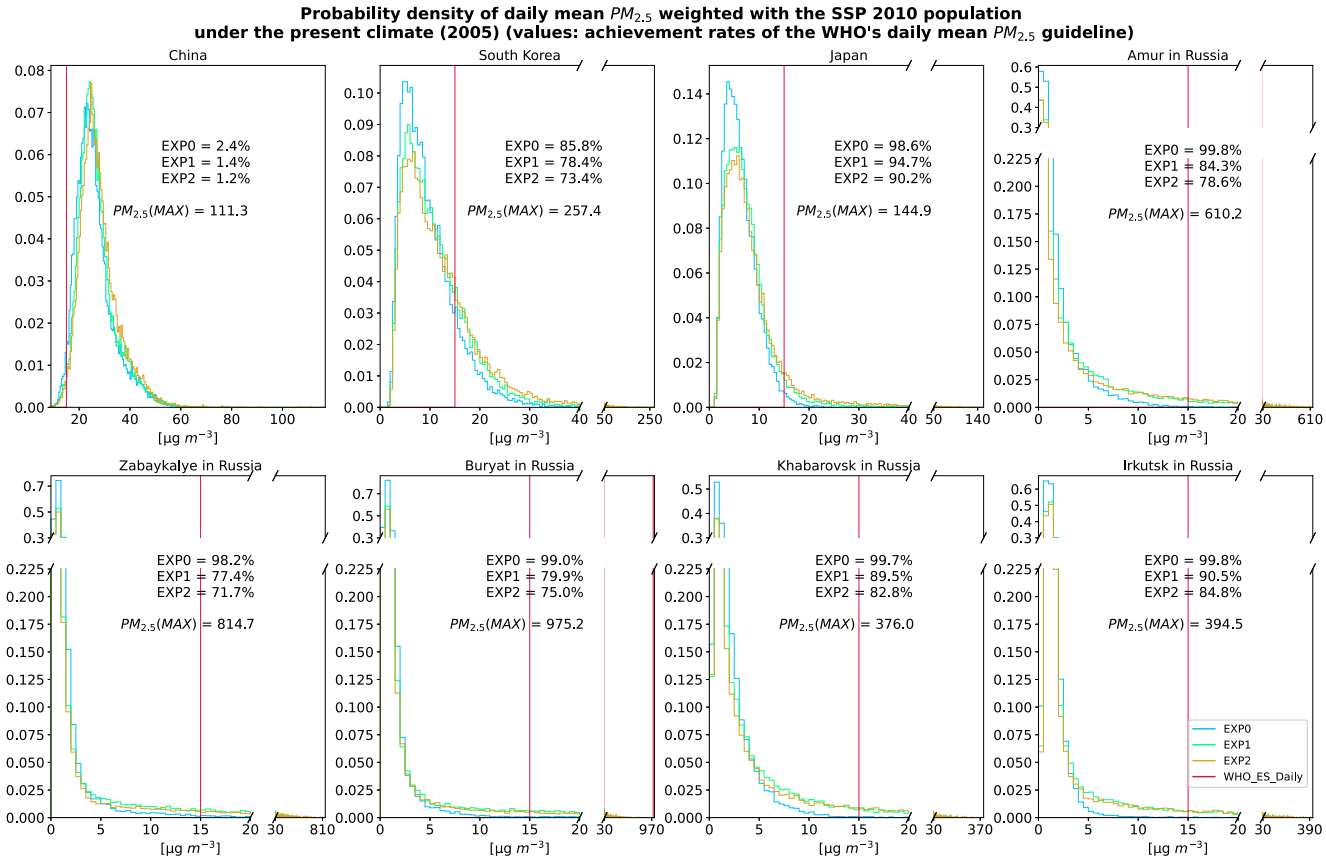


**Figure 2.** Probability density distribution of $PM_{2.5}$ (the SSP 2010 population data weighted $PM_{2.5}$) and percentage of achievement rates satisfying the recent WHO-defined daily mean $PM_{2.5}$ environmental standard (15 μg $m^{-3}$; WHO, 2021) under the present climate conditions (EXPs 0–2; Section 2) in the selected countries and Russian administrative divisions. The daily mean data from the AOGCM experiments were used. The broken axes for the *x* and *y* axes were used to clear the plot differences. Because the ranges of $PM_{2.5}$ are vast, the maximum $PM_{2.5}$ value within the three experiments is also shown. The bin size of the probability density was every 0.5 μg $m^{-3}$.

rate percentages were similar to those under the present climate conditions in our sensitivity assessments (Figure S8 in Supporting Information S1). Next, we analyzed the mortality due to increased Siberian wildfire emissions.

By applying the GEMM (Burnett et al., 2018), an established epidemiological model of the relationship between air pollution and premature human deaths, we estimated the mortality impact of the enhanced Siberian wildfires (Figure 3). They are defined as the difference between the results of EXP2 and EXP0, through $PM_{2.5}$ air pollution, for selected East Asian countries with large economies and populations and Russian administrative districts in the baseline year (2010). Utilizing the widely used approach of assessing the economic costs of pollution-related mortality based on the VSL, the monetary-equivalent losses of excess mortality (welfare losses) were also quantified (circles on the map in Figure 3). The annual excess mortality count was approximately 67,000 for China and 22,000 for Japan, corresponding to approximately 51 billion USD for China and 84 billion USD for Japan. These estimated levels of mortality are substantial in absolute terms but still a relatively small fraction of estimated total counts of excess deaths from air pollution in the region; for example, over 2 million of the total annual excess deaths from $PM_{2.5}$ in China were estimated using the GEMM model (Burnett et al., 2018).

Correspondingly, the small population size in Russian districts in Siberia has resulted in comparatively low levels of mortality. However, nearly 3,000 excess deaths are estimated in the Irkutsk district (Oblast), corresponding to approximately 5 billion USD.

Quantification of the effects of air pollution on mortality is generally subject to various uncertainties in the model and parameters. Therefore, we conducted alternative estimations using the IER model (Burnett et al., 2014). They yielded somewhat different numbers from the GEMM estimations, but the order remained the same (Table S1 in

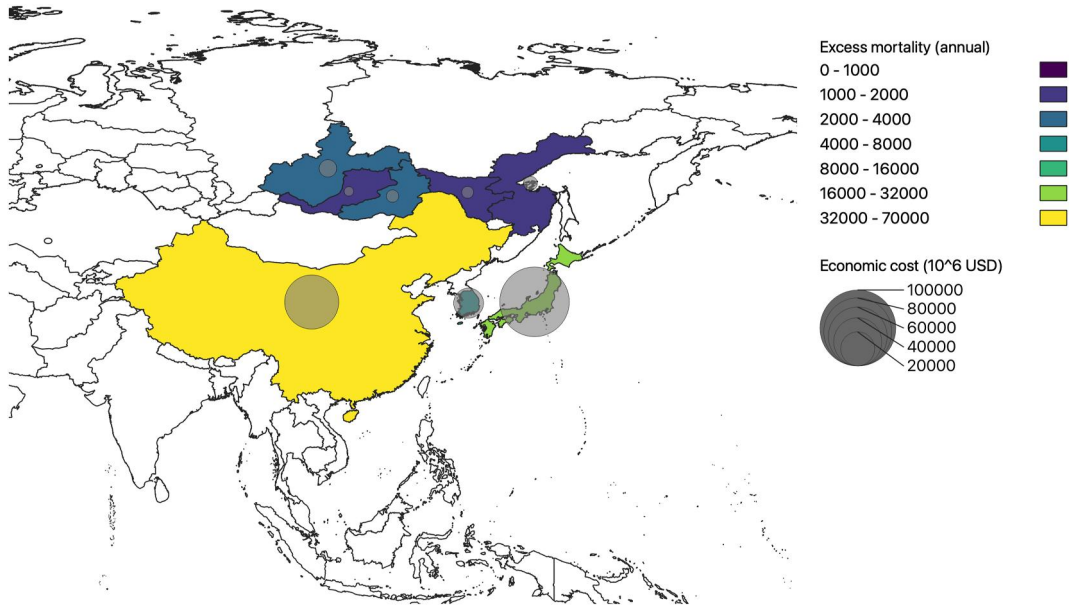


**Figure 3.** Mortality impact of enhanced Siberian wildfires through air pollution (EXP2–EXP0 from the AOGCM experiments) for selected East Asian countries and Russian administrative districts estimated using the GEMM functions. Color shading represents the annual excess mortality due to $PM_{2.5}$ air pollution from increased wildfires (mortality count for country/region), and the circles correspond to the economic cost (welfare loss) from the excess mortality (million 2010 US dollars for country/district). Numerical data corresponding to the circles and colors are presented in Table S1 of the Supporting Information S1.

Supporting Information S1). The GEMM model itself also carries uncertainties, and consequently, our GEMM-based estimates are subject to uncertainties, as shown on Table S1 in Supporting Information S1.

### 3.2. Regional and Global Impact of Increasing Siberian Wildfires on Aerosols and Climate

A substantial cooling effect on IARF at the surface of $<-2.0$ W $m^{-2}$ due to the increased aerosols from the wildfires was observed over the above areas (i.e., negative IARF from the AGCM experiments; here, we used the net radiation of shortwave and longwave radiation for IARF) (Figure S9 in Supporting Information S1). The ERFs at the top of the atmosphere under the fixed sea surface temperature conditions estimated from the AGCM experiments showed significant cooling at a 95% confidence limit (CL) over the Siberian domain under the present climate conditions (EXP1 and EXP2) compared to the baseline case (EXP0) (Figures 4a and 4b and Figures S10a and S10b in Supporting Information S1). Although similar cooling characteristics of ERFs were observed over Siberia, even under the near-future climate conditions in 2030, their global mean values were significantly positive at 99% or 99.9% CL (Figures 4c–4e and Figures S10c–S10e in Supporting Information S1).

The ERFs at the surface showed similar characteristics, but the global mean values under the near-future climate conditions were not significant except for the comparison between EXP3 and EXP0 (95% CL; Figure S11 in Supporting Information S1). Under the present climate conditions, significantly stronger cooling effects of lower than −0.3°C at 2 m (95% CL) are likely over the Siberian wildfire source region (Figures 5a and 5b and Figure S12 in Supporting Information S1). Similar substantial cooling effects were observed in EXP1 and EXP2, such as in the Arctic Ocean and Canadian Arctic, compared to EXP0, respectively. Additionally, cooling bands were observed to be characteristic across the Pacific Ocean from Siberia all the way to North America under the present climate condition (i.e., broad areas of the Northern Hemisphere), corresponding to the areas of increased atmospheric $PM_{2.5}$, namely aerosols (Figure 1). Notably, some significant warming at 95% CL was also observed over the Barents Sea in EXP2–EXP0 (Figure 5b). Under the near-future conditions in 2030, more substantial warming was observed in many regions (Figures 5c–5e). However, the Siberian wildfire source areas, corresponding to areas in the negative ERF, showed no significant warming, likely implying that the increased aerosols contributed to the suppression of warming over the area.

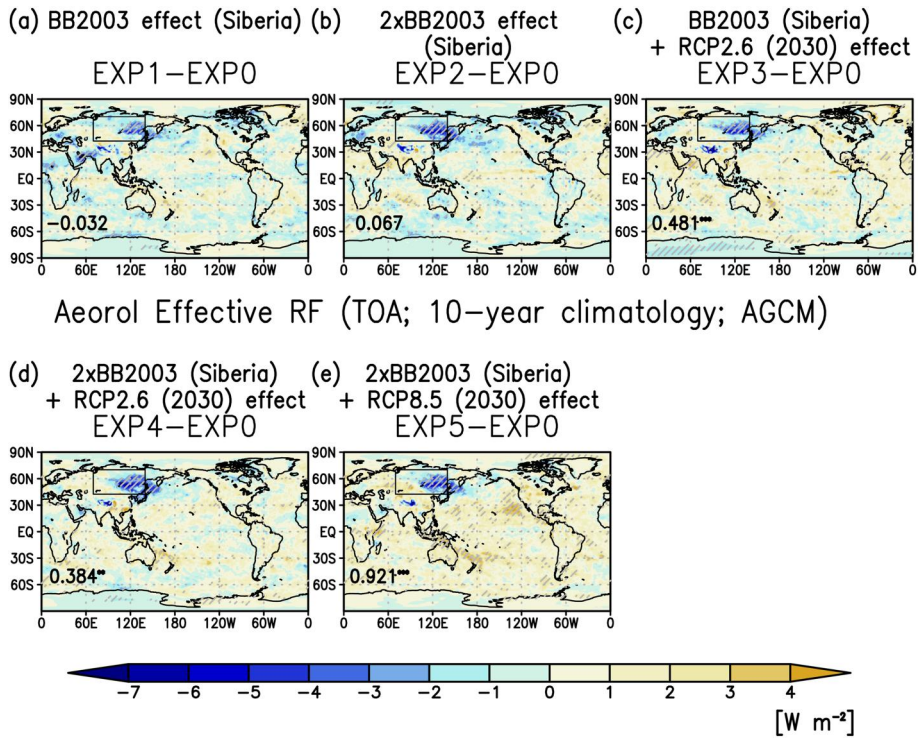


**Figure 4.** Effective radiative forcing (ERF) at the top of the atmosphere based on the AGCM experiments due to the increased Siberian wildfire or the increased Siberian wildfire and global warming (RCP2.6 or RCP8.5). The values and asterisks shown at the bottom left are the global mean values and their confidence limits for the mean differences (CL) of 99% (**) and 99.9% (***), respectively. The hatched areas in the global maps are the CL for the mean differences of 95%. Note that the ERFs in each panel directly reflect the differences between the two focused experiments (i.e., only the impact changes of the Siberian wildfire or the impact changes of the Siberian wildfire and global warming). A similar figure where the region from Siberia to the North Pacific was enlarged is available in Figure S10 of the Supporting Information S1.

### 3.3. Estimated Country-Level Welfare Impact Due To the Increased Siberian Wildfires

Recent economic studies on climate change, such as that by Burke et al. (2018), have identified the statistical relationship between surface temperature and countries' economic performance after controlling for other determinants. These estimations exploit the variabilities of observed weather variables without differentiating their causes, and thus the identified statistical relationships could be applied to assessing economic impacts of various types of climatic changes irrespective of their determinants and patterns, as demonstrated by Zheng et al.'s (2020) study on economic evaluation of general aerosol impacts on climate. Based on this framework, it is possible to estimate the macroeconomic effects of wildfire-originated aerosols (GDP impact) based on their climatic influence. Therefore, we applied the GDP response function of annual surface temperature developed by Burke et al. (2018) and computed the country-level macroeconomic impact (welfare impact) of enhanced Siberian wildfires through climatic effects for selected nations, whose relatively large populations and economies render substantial levels of economic impacts (Figure 6). Drawing on the findings of Burke et al. (2015), the Burke et al.'s function uses the annual average temperature as a proxy for shifting distributions of daily temperatures, the causes of which in the past observational data include aerosol emissions from wildfires. It is also worth noting that wildfires affect the climate not only locally at the time of the event but also at distant locations and times. The upper map in Figure 6 shows the isolated effects of these aerosols through climate change given the baseline present global climate (EXP2–EXP0), while the lower map presents the combined effects of the wildfire-originated aerosols and the other greenhouse gases for the year 2030 (EXP5–EXP0).

As the function described by Burke et al. (2018) assumes an inverse U-shaped relationship between temperature and GDP, temperature reduction due to aerosols may yield different economic impact in different regions of the world. For example, isolated climate-related effects of aerosols from enhanced Siberian wildfires in the baseline

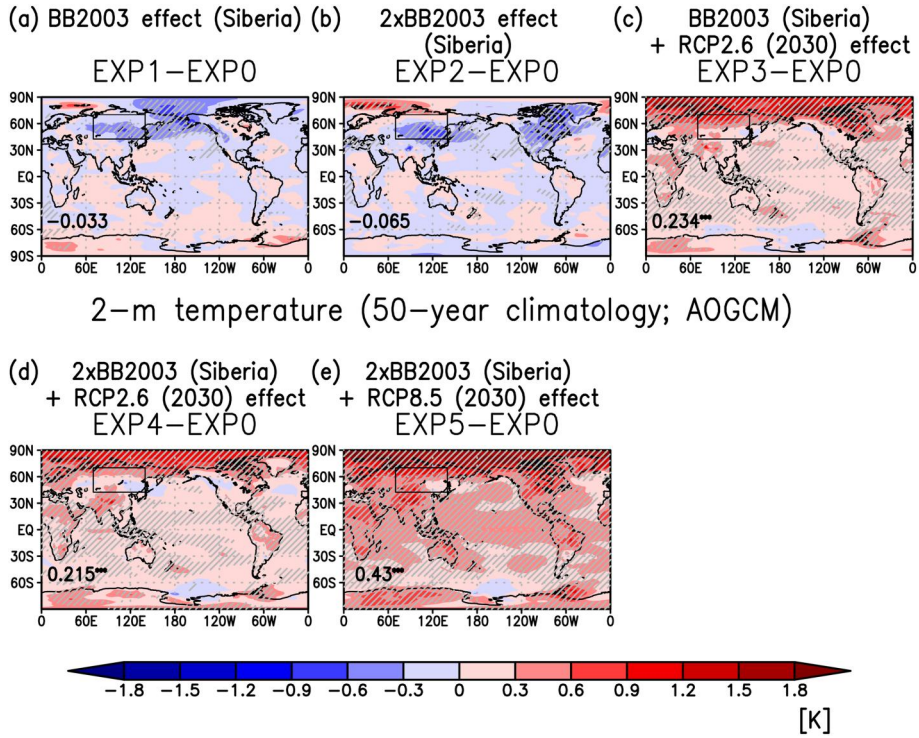


**Figure 5.** Mean differences of 50-year 2-m temperature climatology based on the AOGCM experiments due to the increased Siberian wildfire or the increased Siberian wildfire and global warming (RCP2.6 or RCP8.5). The values and asterisks shown at the bottom left are the global mean values and their confidence limits for the mean differences (CL) of 99.9% (***), respectively. The hatched areas in the global maps are the CL for the mean differences of 95%. A similar figure where the region from Siberia to the North Pacific was enlarged is available in Figure S12 of the Supporting Information S1.

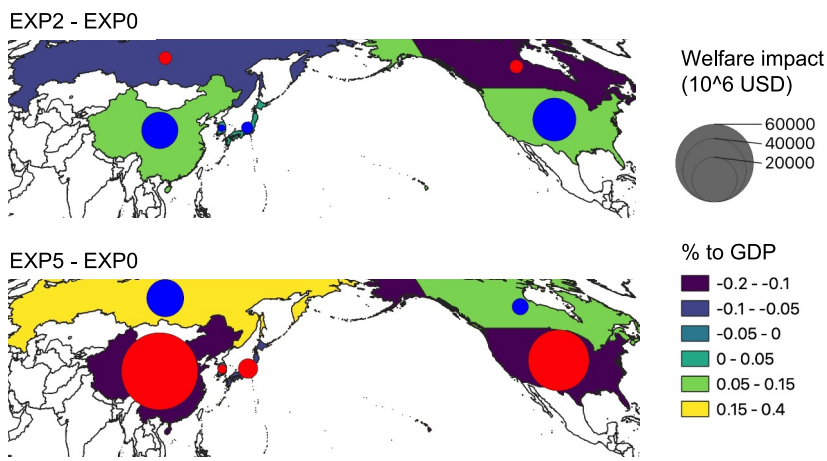


**Figure 6.** Country-level macroeconomic (welfare) impact (in million 2010 US dollars) of enhanced Siberian wildfires through climatic effects for selected nations estimated by using the functions described by Burke et al. (2018). The upper map shows the climatic effects of aerosols at the baseline global climate (EXP2–EXP0; AOGCM experiments), while the lower map presents the combined effects of wildfire-originated aerosols and overall global climate change for the year 2030 (EXP5–EXP0; AOGCM experiments). Blue circles represent positive impact (i.e., cooling causes positive economic effects), and red corresponds to negative impact. Numerical data corresponding to the circles are presented in Table S2 of the Supporting Information S1.

year (EXP2–EXP0) appear as an economic gain in low-latitude countries such as China and the US (approximately 13 billion USD and 19 billion USD annually, respectively), whereas economic losses are found in high-latitude countries such as Russia and Canada. Conversely, the combined climate change effects of wildfire-originated aerosols and other greenhouse gases, including carbon dioxide (EXP5–EXP0), have negative economic consequences for the low-latitude countries (approximately 58 billion USD in China and 36 billion USD in the US annually) and positive consequences for the higher-latitude countries. It should be noted, however, that the Burke et al.'s statistical function carries uncertainties, and consequently, that those monetary estimates are also subject to uncertainties (shown on Table S2 in Supporting Information S1). Overall, the monetary-equivalent pollution and climatic effects of aerosols from enhanced Siberian wildfires were comparable in scale.

## 4. Discussion and Conclusions

Based on our sensitivity experiments using a GCM in Japan, the overall impact of increased Siberian wildfires on climate was a cooling effect due to increased atmospheric aerosols. In terms of climate change, this works to partially suppress global warming in selected near-future scenarios. On the contrary, increased Siberian wildfire aerosols would substantially worsen air quality, especially in the surrounding and downwind regions of Siberia. This directly relates to human mortality and welfare losses near wildfire sources and in downwind regions.

Our estimation of pollution-related mortality from enhanced Siberian wildfires suggests that they could exert substantial health-related costs in Eastern Siberia and East Asia, whose monetary-equivalent values could well be in the order of 10 billion USD annually, as evaluated using the willingness-to-pay method. Note that these figures only account for the direct impact of deaths and not for non-fatal health effects and secondary social impact, such as the loss of educational opportunities due to illness. The results also highlight the fact that climate–economy interactions could be another major type of economic consequence of aerosols from Siberian wildfires. Although the effects are smaller relative to the general trend of global warming due to carbon dioxide and other greenhouse gases, they have some noteworthy features, such as a cooling-induced loss of GDP in Russia and Canada, which are located at high latitudes.

Aerosols emitted from Siberian wildfires act as short-lived climate forcers (SLCFs), affecting the global climate (Szopa et al., 2021). Generally, anthropogenic climate change affects global macroeconomic performance through many pathways, such as intensifying weather extremes and temperature-related yield losses in major crops (Interagency Working Group on Social Cost of Greenhouse Gases, United States Government, 2016; National Academies of Sciences, Engineering, and Medicine, 2017). A wide range of economic studies has been conducted to quantify such impact. One way to synthesize these efforts is to estimate the social cost of carbon (Interagency Working Group on Social Cost of Greenhouse Gases, United States Government, 2016; National Academies of Sciences, Engineering, and Medicine, 2017). This framework has been applied to air pollution (short-lived climate pollutants) by the WMO and UNEP (WHO & UNEP, 2011). As a parallel set of studies, Dell et al. (2012) and Burke et al. (2018) directly investigated the statistical relationships between climatic variables and economic output from past data.

In recent years, due to the reporting of a unique climate pattern, the possibility of the co-occurrence of Siberian wildfires with European heatwaves and wildfires from Alaska and Canada has been suggested (Yasunari et al., 2021). In the future, amplified global warming is likely to cause more wildfires in the extratropics (Veira et al., 2016) and fire weather (IPCC, 2021). Hence, a higher probability of increased Siberian wildfires is expected in the future. This projection means that worse air quality due to wildfires will be likely in the future, which will also likely exceed the air quality ES frequently (i.e., lowering the achievement rates of the short-term $PM_{2.5}$ ES), as shown in Figure S8 of the Supporting Information S1. Thus, we probably need better measures and prediction methods to limit wildfire smoke exposure from the fire source region in Siberia to the downwind region in East Asia. Our estimate is based on limited sensitivity simulations of the GCM considering increased Siberian wildfires under the present and near-future climate conditions.

Although we assessed the comprehensive impact of Siberian wildfires on air quality, climate, mortality, and macroeconomic welfare losses, those were not interactively simulated in the model. For example, the wildfire occurrences in the model were based on a pre-existing BB emission data set. Furthermore, the experiments were only based on single global model simulations. Therefore, a natural extension of this study in the future would be an analysis with an interactive global model. Such an analysis should use, for example, an interactive wildfire model (Veira et al., 2016), which draws on more experiments from various global model outputs. A similar

analysis was performed in a recent study estimating the global mortality due to ozone and $PM_{2.5}$ using the ensemble of global climate simulations (Silva et al., 2017).

Despite the limitations of our study, our findings provide readers with a critical message on the effect of increased particulate matter due to Siberian wildfires on climate and air quality as well as mortality and the economy under present and future atmospheric conditions. The MIROC5's climate reproducibility was confirmed within a reasonable range under the Coupled Model Intercomparison Project Phase 5 (CMIP5) in the fifth IPCC report, compared to the other climate models used in CMIP5 (Flato et al., 2013). In the Atmospheric Chemistry and Climate Model Intercomparison Project (ACCMIP), the aerosol performance of MIROC5 in the comparisons with the global ground-based aerosol optical depth observations also quantitatively showed reasonable statistical values within the multi-model comparisons (e.g., see Table G1 of Shindell et al. (2013)). Therefore, we consider that our results from the MIROC5/SPRINTARS sensitivity experiments also showed reasonable and general characteristics of Siberian wildfires and their aerosols ($PM_{2.5}$) from one of the known climate models used in the world. Future studies must aim to prevent air pollution emissions from Siberian wildfires and take further preventive measures in the future under ongoing and future climate changes (IPCC, 2021).

## Conflict of Interest

The authors declare no conflicts of interest relevant to this study.

## Data Availability Statement

The modeling-related data, codes, and scripts for the calculations and plots used in this study, including large data sets from global climate simulations, were archived in Zenodo (Yasunari et al., 2024: v4.0). Some of the following publicly available data we used in the paper were also archived together in the Zenodo data repository (see Yasunari et al., 2024). The other publicly available data mentioned in Section 2 (Materials and Methods) are as follows: the Global Fire Emission Database (GFED; version 3.1; https://www.globalfiredata.org/) (Randerson et al., 2013; van der Werf et al., 2010), which was used for the global climate model simulations; the population data provided by the Shared Socioeconomic Pathways (SSP) (Riahi et al., 2017) (Version 1.0; https://secure.iiasa.ac.at/web-apps/ene/SspDb/dsd?Action=htmlpage&page=10); the World Population Prospects 2019 data from the United Nations (https://www.un.org/development/desa/pd/news/world-population-prospects-2019-0); the mortality data from the Centre for Demographic Research at the New Economic School (http://demogr.nes.ru/en/demogr_indicat/data); the economic data of the Russian Federal State Statistic Service (https://rosstat.gov.ru); The monthly mean global data-assimilated $PM_{2.5}$ (V5.GL.04) based on the chemical transport model and observations are publicly available at https://sites.wustl.edu/acag/datasets/surface-pm2-5/#V5.GL.04.

**Acknowledgments**

This study was partially supported by the Arctic Challenge for Sustainability (ArCS) project (JPMXD1300000000) and its following project, ArCS II (JPMXD1420318865), of the Ministry of Education, Culture, Sports, Science and Technology in Japan; Grant-in-Aid for Scientific Research (B) (JSPS KAKENHI Grants JP17KT0066, JP19H01976, and JP24K00711), (A) (Grant JP15H01728), and (S) (Grant JP19H05669); Supercomputer system of the National Institute for Environmental Studies, Japan; and Environment Research and Technology Development Fund (S-20 (JPMEERF21S12010), 2-1803, and 2-2201) of the Environmental Restoration and Conservation Agency of Japan. We would like to thank Editage (www.editage.com) for the English language editing.

## References

Aguilera, R., Corringham, T., Gershunov, A., & Benmarhnia, T. (2021). Wildfire smoke impacts respiratory health more than fine particles from other sources: Observational evidence from Southern California. *Nature Communications*, *12*(1), 1493. https://doi.org/10.1038/s41467-021-21708-0

Amatulli, G., Peréz-Cabello, F., & de la Riva, J. (2007). Mapping lightning/human-caused wildfires occurrence under ignition point location uncertainty. *Ecological Modelling*, *200*(3–4), 321–333. https://doi.org/10.1016/j.ecolmodel.2006.08.001

Burke, M., Davis, W. M., & Diffenbaugh, N. S. (2018). Large potential reduction in economic damages under UN mitigation targets. *Nature*, *557*(7706), 549–553. https://doi.org/10.1038/s41586-018-0071-9

Burke, M., Hsiang, S. M., & Miguel, E. (2015). Global non-linear effect of temperature on economic production. *Nature*, *527*(7577), 235–239. https://doi.org/10.1038/nature15725

Burnett, R., Chen, H., Szyszkowicz, M., Fann, N., Hubbell, B., Pope, C. A., III., et al. (2018). Global estimates of mortality associated with long-term exposure to outdoor fine particulate matter. *Proceedings of the National Academy of Sciences of the United States of America*, *115*(38), 9592–9597. https://doi.org/10.1073/pnas.1803222115

Burnett, R. T., Pope, C. A., III., Ezzati, M., Olives, C., Lim, S. S., Mehta, S., et al. (2014). An integrated risk function for estimating the global burden of disease attributable to ambient fine particulate matter exposure. *Environmental Health Perspectives*, *122*(4), 397–403. https://doi.org/10.1289/ehp.1307049

Cohen, A. J., Brauer, M., Burnett, R., Anderson, H. R., Frostad, J., Estep, K., et al. (2017). Estimates and 25-year trends of the global burden of disease attributable to ambient air pollution: An analysis of data from the Global Burden of Diseases Study 2015. *Lancet*, *389*(10082), 1907–1918. https://doi.org/10.1016/S0140-6736(17)30505-6

Darmenov, A., & da Silva, A. (2015). *The quick fire emissions dataset (QFED): Documentation of versions. 2.2 and 2.4* (Vol. 2). National Aeronautics and Space Administration/TM–2015–104606 38. Retrieved from https://gmao.gsfc.nasa.gov/pubs/docs/Darmenov796.pdf

Dell, M., Jones, B. F., & Olken, B. A. (2012). Temperature shocks and economic growth: Evidence from the last half century. *American Economic Journal: Macroeconomics*, *4*(3), 66–95. https://doi.org/10.1257/mac.4.3.66

Flanner, M. G., Zender, C. S., Hess, P. G., Mahowald, N. M., Painter, T. H., Ramanathan, V., & Rasch, P. J. (2009). Springtime warming and reduced snow cover from carbonaceous particles. *Atmospheric Chemistry and Physics*, *9*(7), 2481–2497. https://doi.org/10.5194/acp-9-2481-2009

Flato, G., Marotzke, J., Abiodun, B., Braconnot, P., Chou, S. C., Collins, W., et al. (2013). Evaluation of climate models. In T. F. Stocker, et al. (Ed.), *Climate change 2013: The physical science basis. Contribution of working group I to the fifth assessment report of the intergovernmental panel on climate change* (pp. 741–866). Cambridge University Press. Retrieved from https://www.ipcc.ch/report/ar5/wg1/

Forster, P. M., Richardson, T., Maycock, A. C., Smith, C. J., Samset, B. H., Myhre, G., et al. (2016). Recommendations for diagnosing effective radiative forcing from climate models for CMIP6. *Journal of Geophysical Research: Atmospheres*, *121*(20), 12–460. https://doi.org/10.1002/2016JD025320

GBD 2015 Risk Factors Collaborators. (2016). Global, regional, and national comparative risk assessment of 79 behavioural, environmental and occupational, and metabolic risks or clusters of risks, 1990–2015: A systematic analysis for the Global Burden of Disease Study 2015. *Lancet*, *388*, 1659–1724. https://doi.org/10.1016/S0140-6736(16)31679-8

GBD 2017 SDG Collaborators. (2018). Measuring progress from 1990 to 2017 and projecting attainment to 2030 of health-related sustainable development goals for 195 countries and territories: A systematic analysis for the Global Burden of Disease Study 2017. *Lancet*, *392*, 2091–2138. https://doi.org/10.1016/S0140-6736(18)32281-5

Ikeda, K., & Tanimoto, H. (2015). Exceedances of air quality standard level of $PM_{2.5}$ in Japan caused by Siberian wildfires. *Environmental Research Letters*, *105001*(10), 105001. https://doi.org/10.1088/1748-9326/10/10/105001

Interagency Working Group on Social Cost of Greenhouse Gases, United States Government. (2016). Technical support document: Technical update of the social cost of carbon for regulatory impact analysis under executive order 12866. Retrieved from https://www.epa.gov/sites/default/files/2016-12/documents/sc_co2_tsd_august_2016.pdf

IPCC. (2021). Summary for policymakers. In V. Masson-Delmotte, P. Zhai, A. Pirani, S. L. Connors, C. Péan, S. Berger, et al. (Eds.), *Climate change 2021: The physical science basis. Contribution of working group I to the sixth assessment report of the intergovernmental panel on climate change* (pp. 3–32). Cambridge University Press. https://doi.org/10.1017/9781009157896.001

Kochi, I., Champ, P. A., Loomis, J. B., & Donovan, G. H. (2012). Valuing mortality impacts of smoke exposure from major Southern California wildfires. *Journal of Forest Economics*, *18*(1), 61–75. https://doi.org/10.1016/j.jfe.2011.10.002

Landrigan, P. J., Fuller, R., Acosta, N. J. R., Adeyi, O., Arnold, R., Basu, N. N., et al. (2018). The Lancet Commission on pollution and health. *Lancet*, *391*(10119), 462–512. https://doi.org/10.1016/S0140-6736(17)32345-0

Lelieveld, J., Evans, J. S., Fnais, M., Giannadaki, D., & Pozzer, A. (2015). The contribution of outdoor air pollution sources to premature mortality on a global scale. *Nature*, *525*(7569), 367–371. https://doi.org/10.1038/nature15371

Liu, Y., Goodrick, S., & Heilman, W. (2014). Wildland fire emissions, carbon, and climate: Wildfire–climate interactions. *Forest Ecology and Management*, *317*, 80–96. https://doi.org/10.1016/j.foreco.2013.02.020

Moss, R. H., Edmonds, J. A., Hibbard, K. A., Manning, M. R., Rose, S. K., van Vuuren, D. P., et al. (2010). The next generation of scenarios for climate change research and assessment. *Nature*, *463*(7282), 747–756. https://doi.org/10.1038/nature08823

Myhre, G., Shindell, D., Bréon, F.-M., Collins, W., Fuglestvedt, J., Huang, J., et al. (2013). Anthropogenic and natural radiative forcing. In T. F. Stocker, et al. (Eds.), *Climate change 2013: The physical science basis. Contribution of working group I to the fifth assessment report of the intergovernmental panel on climate change* (pp. 659–740). Cambridge University Press. Retrieved from https://www.ipcc.ch/report/ar5/wg1/

Narain, U., & Sall, C. (2016). Methodology for valuing the health impacts of air pollution: Discussion of challenges and proposed solutions. *Environment Department Papers*. World Bank. https://doi.org/10.1596/24440

Narita, D., Gavrilyeva, T., & Isaev, A. (2021). Impacts and management of forest fires in the Republic of Sakha, Russia: A local perspective for a global problem. *Polar Science*, *27*, 100573. https://doi.org/10.1016/j.polar.2020.100573

National Academies of Sciences, Engineering, and Medicine. (2017). Valuing climate damages: Updating estimation of the social cost of carbon dioxide. *Consensus Study Report*. The National Academies Press. Retrieved from https://nap.nationalacademies.org/catalog/24651/valuing-climate-damages-updating-estimation-of-the-social-cost-of

Pan, X., Ichoku, C., Chin, M., Bian, H., Darmenov, A., Colarco, P., et al. (2020). Six global biomass burning emission datasets: Intercomparison and application in one global aerosol model. *Atmospheric Chemistry and Physics*, *20*(2), 969–994. https://doi.org/10.5194/acp-20-969-2020

Randerson, J. T., van der Werf, G. R., Giglio, L., Collatz, G. J., & Kasibhatla, P. S. (2013). Global fire emissions database, version 3.1 [Dataset]. *ORNL DAAC*. https://doi.org/10.3334/ORNLDAAC/1191

Riahi, K., van Vuuren, D. P., Kriegler, E., Edmonds, J., O'Neill, B. C., Fujimori, S., et al. (2017). The shared socioeconomic pathways and their energy, land use, and greenhouse gas emissions implications: An overview. *Global Environmental Change*, *42*, 153–168. https://doi.org/10.1016/j.gloenvcha.2016.05.009

Rodrigues, M., & de la Riva, J. (2014). An insight into machine-learning algorithms to model human-caused wildfire occurrence. *Environmental Modelling & Software*, *57*, 192–201. https://doi.org/10.1016/j.envsoft.2014.03.003

Scovronick, N., Budolfson, M., Dennig, F., Errickson, F., Fleurbaey, M., Peng, W., et al. (2019). The impact of human health co-benefits on evaluations of global climate policy. *Nature Communications*, *10*(1), 2095. https://doi.org/10.1038/s41467-019-09499-x

Seposo, X., Ueda, K., Park, S. S., Sudo, K., Takemura, T., & Nakajima, T. (2019). Effect of global atmospheric aerosol emission change on $PM_{2.5}$-related health impacts. *Global Health Action*, *12*(1), 1664130. https://doi.org/10.1080/16549716.2019.1664130

Shaposhnikov, D., Revich, B., Bellander, T., Bedada, G. B., Bottai, M., Kharkova, T., et al. (2014). Mortality related to air pollution with the Moscow heat wave and wildfire of 2010. *Epidemiology*, *25*(3), 359–364. https://doi.org/10.1097/EDE.0000000000000090

Shindell, D. T. (2015). The social cost of atmospheric release. *Climate Change*, *130*(2), 313–326. https://doi.org/10.1007/s10584-015-1343-0

Shindell, D. T., Lamarque, J.-F., Schulz, M., Flanner, M., Jiao, C., Chin, M., et al. (2013). Radiative forcing in the ACCMIP historical and future climate simulations. *Atmospheric Chemistry and Physics*, *13*(6), 2939–2974. https://doi.org/10.5194/acp-13-2939-2013

Silva, R. A., West, J. J., Lamarque, J. F., Shindell, D. T., Collins, W. J., Faluvegi, G., et al. (2017). Future global mortality from changes in air pollution attributable to climate change. *Nature Climate Change*, *7*(9), 647–651. https://doi.org/10.1038/nclimate3354

Szopa, S., Naik, V., Adhikary, B., Artaxo, P., Berntsen, T., Collins, W. D., et al. (2021). Short-lived climate forcers. In V. Masson-Delmotte, et al. (Eds.), *Climate change 2021: The physical science basis. Contribution of working group I to the sixth assessment report of the intergovernmental panel on climate change* (pp. 817–922). Cambridge University Press. https://doi.org/10.1017/9781009157896.008

Takemura, T., Nakajima, T., Dubovik, O., Holben, B. N., & Kinne, S. (2002). Single-scattering albedo and radiative forcing of various aerosol species with a global three-dimensional model. *Journal of Climate*, *15*(4), 333–352. https://doi.org/10.1175/1520-0442(2002)015<0333:SSAARF>2.0.CO;2

Takemura, T., Okamoto, H., Maruyama, Y., Numaguti, A., Higurashi, A., & Nakajima, T. (2000). Global three-dimensional simulation of aerosol optical thickness distribution of various origins. *Journal of Geophysical Research*, *105*(D14), 17853–17873. https://doi.org/10.1029/2000JD900265

van der Werf, G. R., Randerson, J. T., Giglio, L., Collatz, G. J., Mu, M., Kasibhatla, P. S., et al. (2010). Global fire emissions and the contribution of deforestation, savanna, forest, agricultural, and peat fires (1997–2009). *Atmospheric Chemistry and Physics*, *10*(23), 11707–11735. https://doi.org/10.5194/acp-10-11707-2010

van Donkelaar, A., Hammer, M. S., Bindle, L., Brauer, M., Brook, J. R., Garay, M. J., et al. (2021). Monthly global estimates of fine particulate matter and their uncertainty. *Environmental Science and Technology*, *55*(22), 15287–15300. https://doi.org/10.1021/acs.est.1c05309

van Vuuren, D. P., Edmonds, J., Kainuma, M., Riahi, K., Thomson, A., Hibbard, K., et al. (2011). The representative concentration pathways: An overview. *Climatic Change*, *109*(1–2), 5–31. https://doi.org/10.1007/s10584-011-0148-z

Veira, A., Lasslop, G., & Kloster, S. (2016). Wildfires in a warmer climate: Emission fluxes, emission heights, and black carbon concentrations in 2090–2099. *Journal of Geophysical Research: Atmospheres*, *121*(7), 3195–3223. https://doi.org/10.1002/2015JD024142

Wang, D., Guan, D., Zhu, S., Kinnon, M. M., Geng, G., Zhang, Q., et al. (2021). Economic footprint of California wildfires in 2018. *Nature Sustainability*, *4*(3), 252–260. https://doi.org/10.1038/s41893-020-00646-7

Watanabe, M., Suzuki, T., O'ishi, R., Komuro, Y., Watanabe, S., Emori, S., et al. (2010). Improved climate simulation by MIROC5: Mean states, variability, and climate sensitivity. *Journal of Climate*, *23*(23), 6312–6335. https://doi.org/10.1175/2010JCLI3679.1

Westerling, A. L., & Bryant, B. P. (2008). Climate change and wildfire in California. *Climatic Change*, *87*(S1), 231–249. https://doi.org/10.1007/s10584-007-9363-z

Westerling, A. L., Hidalgo, H. G., Cayan, D. R., & Swetnam, T. W. (2006). Warming and earlier spring increase Western U.S. forest wildfire activity. *Science*, *313*(5789), 940–943. https://doi.org/10.1126/science.1128834

World Bank, & Institute for Health Metrics and Evaluation. (2016). *The cost of air pollution: Strengthening the economic case for action*. World Bank. Retrieved from http://hdl.handle.net/10986/25013

World Health Organization (WHO). (2021). WHO global air quality guidelines: Particulate matter ($PM_{2.5}$ and $PM_{10}$), ozone, nitrogen dioxide, sulfur dioxide and carbon monoxide. Retrieved from https://www.who.int/publications/i/item/9789240034228

World Health Organization (WHO). Occupational and Environmental Health Team. (2006). *WHO air quality guidelines for particulate matter, ozone, nitrogen dioxide and sulfur dioxide: Global update 2005. Summary of risk assessment*. World Health Organization. Retrieved from https://apps.who.int/iris/handle/10665/69477

World Health Organization (WHO), & UNEP. (2011). Integrated assessment of black carbon and tropospheric ozone. Retrieved from https://library.wmo.int/index.php?lvl=notice_display&id=12414#.YcVy7xPP3zc

Yan, H., Zhu, Z., Wang, B., Zhang, K., Luo, J., Qian, Y., & Jiang, Y. (2021). Tropical African wildfire aerosols trigger teleconnections over mid-to-high latitudes of Northern Hemisphere in January. *Environmental Research Letters*, *16*(3), 034025. https://doi.org/10.1088/1748-9326/abe433

Yasunari, T. J., Kim, K. M., da Silva, A. M., Hayasaki, M., Akiyama, M., & Murao, N. (2018). Extreme air pollution events in Hokkaido, Japan, traced back to early snowmelt and large-scale wildfires over East Eurasia: Case studies. *Scientific Reports*, *8*(1), 6413. https://doi.org/10.1038/s41598-018-24335-w

Yasunari, T. J., Nakamura, H., Kim, K. M., Choi, N., Lee, M. I., Tachibana, Y., & da Silva, A. M. (2021). Relationship between circum-Arctic atmospheric wave patterns and large-scale wildfires in boreal summer. *Environmental Research Letters*, *16*(6), 064009. https://doi.org/10.1088/1748-9326/abf7ef

Yasunari, T. J., Narita, D., Takemura, T., Wakabayashi, S., & Takeshima, A. (2024). Data for the submitted paper by Yasunari et al., "Comprehensive impact of changing Siberian wildfire severities on air quality, climate, and economy: MIROC5 global climate model's sensitivity assessments" (v4.0) [Dataset]. *Zenodo*. https://doi.org/10.5281/zenodo.7784059

Yasunari, T. J., Wakabayashi, S., Matsumi, Y., & Matoba, S. (2022). Developing an insulation box with automatic temperature control for $PM_{2.5}$ measurements in cold regions. *Journal of Environmental Management*, *311*, 114784. https://doi.org/10.1016/j.jenvman.2022.114784

Zheng, S., Schlink, U., Ho, K.-F., Singh, R. P., & Pozzer, A. (2021). Spatial distribution of $PM_{2.5}$-related premature mortality in China. *GeoHealth*, *5*(12), e2021GH000532. https://doi.org/10.1029/2021GH000532

Zheng, Y., Davis, S. J., Persad, G. G., & Caldeira, K. (2020). Climate effects of aerosols reduce economic inequality. *Nature Climate Change*, *10*(3), 220–224. https://doi.org/10.1038/s41558-020-0699-y